Experimental Observation and Analysis of Ionosphere Echoes in the Mid-Latitude Region of China Using High-Frequency Surface Wave Radar and Ionosonde

Xuguang Yang, Mingjie Wang, Weimin Huang, *Senior Member, IEEE*, and Changjun Yu

***Abstract*—Ionospheric clutter is a major factor affecting the performance of high-frequency surface wave radar (HFSWR). Previous studies have been mainly focused on the development of ionospheric clutter suppression methods involving delicate signal processing techniques or additional antennas. However, ionospheric clutter originates from the interaction between HF waves and the ionosphere, thus it contains the characteristics of the latter. Therefore, ionospheric clutter can be analyzed to obtain the parameters of the reflecting ionosphere, expanding the value of HFSWR. This article presents the preliminary coordinated observation and analysis results of the characteristics of the ionosphere at mid-latitudes of China using both HFSWR and ionosonde. The results demonstrate the existence of an oblique skywave propagation path (0.5 jump, 1 jump, etc.) in addition to the vertical reflection path and ionosphere-ocean mixed path. HFSWR beams were also found split into an O-trace and an X-trace after entering the ionosphere. Furthermore, range-folded ionospheric echoes are related to the short-term thickening of the F2-layer, showing strong fluctuation in the range-Doppler spectrum of HFSWR. These observed characteristics of ionospheric echoes are useful for the development of an efficient ionospheric clutter suppression algorithm for HFSWR and further investigation of the ionospheric mechanisms at mid-latitudes.**

***Index Terms*—High-frequency surface wave radar (HFSWR), ionosonde, ionospheric clutter.**

I. Introduction

HIGH-FREQUENCY surface wave radar (HFSWR) can detect targets beyond the horizon due to the mechanism of high-frequency wave diffraction along the ocean surface [1]–[6]. Ideally, the radar beam should travel entirely along the ocean surface. However, due to the limitations of radar antenna systems, namely, imperfection of radiation pattern, poor ground, and wind-induced antenna motions, some transmitted waves traveling upward into the ionosphere are reflected along various paths back to the radar receiving system under certain conditions. Such echo is referred to as ionospheric clutter [7], [8]. On one hand, ionospheric clutter often contaminates the radar range-Doppler (RD) spectrum, severely reducing the performance of the HFSWR system, especially for low-frequency, and long-range detection or during nighttime operations. As ionospheric clutter constitutes the major limitation of HFSWR, many ionospheric clutter suppression methods involving smart signal processing techniques or additional antennas have been proposed [9]–[17]. On the other hand, ionospheric clutter originating from the interaction between HF electromagnetic waves and ionosphere certainly contains the characteristics of the latter. Therefore, the ionospheric clutter can also be investigated to obtain the parameters of the reflecting ionosphere to add the value of HFSWR [18]–[21].

In this article, we operate HFSWR and ionosonde alternately to observe the characteristics of the ionosphere in the mid-latitude region of China. Although similar experiments were performed earlier, the corresponding results were only focused on the ionospheric sporadic-E (Es) clutter for HFSWR surveillance in the Arctic environment [22], and the results demonstrated that the main types of Es are thin Es and height-spread Es. Thin Es, which often exhibits a thickness of approximately 15 km, takes the form of a flat yet intense layer that obstructs signal penetration. This type of E-layer is weak but broadly distributed, and thus occupies numerous RD bins in the radar spectra due to the overhead null in the radar antenna pattern. Height-spread Es appears to extend over a range of heights, probably in the form of patches migrating with gases. This type of layer may cause more interference for HFSWR because the signal disperses after being reflected and hence may not be present in the overhead null of the radar antenna pattern.

We implemented a similar experiment setup which includes a digital ionosonde that can separate ordinary and extraordinary traces (O-traces and X-traces, respectively) of ionosphere-reflected electromagnetic waves and an HFSWR to investigate

Manuscript received April 29, 2020; revised June 23, 2020 and July 25, 2020; accepted August 1, 2020. Date of publication August 6, 2020; date of current version August 24, 2020. This work was supported in part by the National Natural Science Foundations of China under Grant 61801141 and Grant 61971159, and in part by Doctoral Fund Project of Longdong University under Grant XYBY202001. *(Corresponding author: Xuguang Yang.)*

Xuguang Yang and Mingjie Wang are with the School of Information Engineering, Long Dong University, Qingyang 745000, China (e-mail: yangxghit@163.com; xiaowangiii@yahoo.com).

Weimin Huang is with the Faculty of Engineering and Applied Science, Memorial University, St. John's, NL A1B 3X5, Canada (e-mail: weimin@mun.ca).

Changjun Yu is with the School of Information Science and Engineering, Harbin Institute of Technology (Weihai), Shandong 294209, China (e-mail: yuchangjun@hit.edu.cn).

Digital Object Identifier 10.1109/JSTARS.2020.3014666

TABLE I
OPERATING PARAMETERS OF THE HFSWR

Coherent processing interval (min)	Sweep period (MS)	Pulse repetition period (ms)	Pulse width (ms)	Peak transmitting power (kW)	Bandwidth (kHz)	Range resolution (km)
5	110	3.45	0.45	2	30	5

the characteristics of both E-layer and F-layer in the mid-latitude region of China. Different from [22], the goals of this study include the following.

1) To confirm the existence of HFSWR ionospheric echoes due to skywave propagation paths [24] in addition to the vertical reflection path and ionosphere-ocean mixed path [23], [25], [26]. Some researchers proposed four possible propagation paths involving the combination of all ground-wave paths and skywave paths [27]–[29]. The identification of actual propagation paths is crucial because the ionospheric clutter suppression algorithms for HFSWR significantly depend on those paths. Many studies about paths of ionospheric echoes are based on theoretical assumptions without experimental validation. In this work, field data from both HFSWR and Ionosonde will be used to verify the existence of skywave propagation path.
2) To investigate the O-trace and X-trace problems from the perspective of HFSWR data. The O-trace and X-trace may display different characteristics in HFSWR spectra and ionograms. A combination of HFSWR and ionosonde measurements can provide more details regarding the characteristics of the ionosphere from different perspectives, which can provide a better understanding of ionospheric mechanisms.
3) To explore the mechanism that leads to range-folded ionospheric echoes in HFSWR spectra. The range-folded ionospheric echoes have indeed been reported by Ponsford *et al.* [34] without validation using Ionosonde data. In this article, we will investigate the ionosphere phenomenon that causes the range-folded ionospheric echoes in HF radar Doppler spectra based on both HF radar data and ionograms.

The rest of the article is organized as follows. Section II introduces the experimental setup. The coordinated HFSWR and ionosonde results and analysis are presented in Section III. The article is concluded in Section IV.

II. EXPERIMENTAL EQUIPMENTS

The HFSWR and ionosonde data used here were both collected from the radar station in Weihai, Shandong Province (37.5 °N, 122 °E). The distance between the HFSWR and ionosonde is less than 1 km. The ionosonde and HFSWR were operated alternately to avoid interference in the same frequency band.

The HFSWR employs a log-periodic transmitting antenna and a receive an array of eight elements that can operate at 3–10 MHz. For the radar signal waveform, the frequency-modulated pulsed continuous wave is selected. The operating parameters of the radar system are shown in Table I. Pulse decompression is carried out after the radar echo signals enter the receiving array to obtain the range information of targets, and a fast Fourier transform is performed in the same distance bins to obtain Doppler bins. In this way, the RD spectrum is generated. Additionally, digital beamforming is implemented to provide an azimuthal coverage over the angles from –60° to 60°.

The ionosonde, which was developed by the 22nd Research Institute of China Electronic Technology Corporation, has two detection modes: a sweep mode at 1–30 MHz and a fixed-frequency detection mode using a delta antenna. The height resolution of the ionosonde is $\leq$5 km; its height accuracy is $\leq$2.5 km; the success rate of separating the polarization of the O/X-traces is $\geq$95%, and the automatic interpretation accuracy for f_0 F2 is $\geq$90%. The ionosonde can also provide other ionospheric parameters, such as the virtual height, estimated real height, and the critical frequencies of the E-layer, F1-layer, and F2-layer (f_0E, f_0F1, and f_0F2, respectively).

III. RESULTS AND DISCUSSION

A. Existence of Skywave Propagation Path for HFSWR

Fig. 1 shows the measured data from the HFSWR and ionosonde at 10:53 A.M. on June 28, 2018 (local time, the same hereafter). The green and red traces in Fig. 1(a) represent the O-traces and X-traces, respectively, and the color bar indicates the echo intensity. Obviously, the E-layer appears at approximately 110–130 km, and f_0E is approximately 5 MHz. The vertical reflection range of 6 MHz in the F-layer is approximately 350 km.

The RD spectrum of HFSWR is shown in Fig. 1(b). The radar operating frequency is 6 MHz, which is higher than f_0E. Strips of ionospheric echoes with high intensity appear at 160–200 km. These ionospheric echoes can be inferred as oblique reflection echoes from the E-layer. However, additional ionospheric echoes can be observed at approximately 400 km and they are associated with secondary reflections. Therefore, for HFSWR, we can conclude that there may exist an oblique skywave path in addition to the vertical reflection path and mixed path. An earlier study further showed that ionospheric clutter can be divided into near-vertical-incidence clutter and range-folded clutter [34]. The Doppler spectrum corresponding to a relatively low pulse repetition frequency (PRF) is much cleaner with distinct Bragg lines and lower noise than that obtained at a high PRF. Additionally, by employing a split complementary P4 code as a transmitting waveform to overcome range ambiguity, HFSWR can even detect targets at a distance of 1000 km via the skywave propagation path, similar to over-the-horizon radar (OTHR) [27].

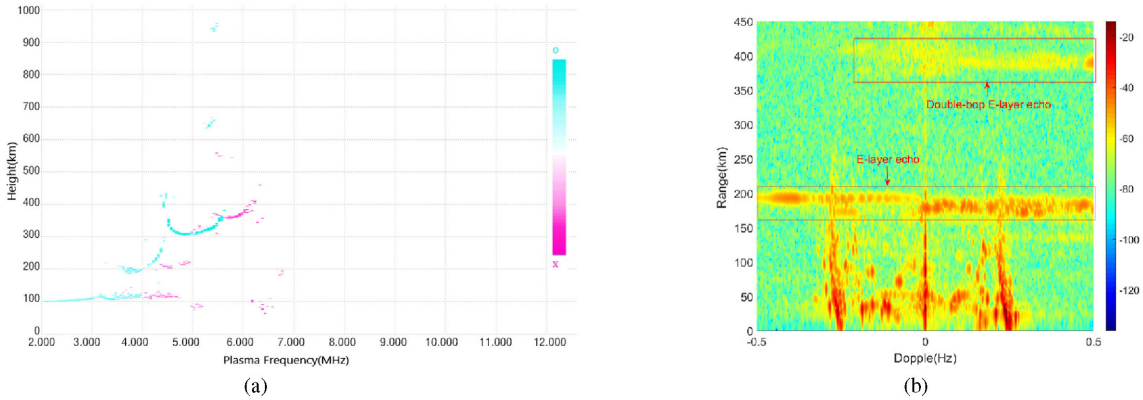

Fig. 1. Comparison between the ionogram and RD spectrum at 10:53 A.M. on June 28, 2018. (a) Ionogram. The vertical axis is the virtual height of the ionosphere, while the horizontal axis is the plasma frequency. (b) RD spectrum of HFSWR. The vertical axis is the range from the radar to the target, while the horizontal axis is the Doppler frequency of the target.

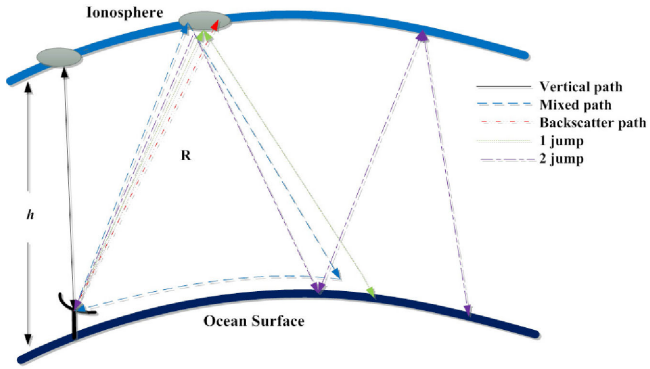

Fig. 2. Possible propagation paths of ionospheric echoes for HFSWR.

In summary, there are two types of ionospheric echo propagation paths: one is the skywave path passing through the ionosphere, and the other is the mixed path involving both the ionosphere and the ocean surface. The skywave path can be divided into vertical and oblique reflections. According to the definition of the skywave propagation path, the path with backscattering directly from the ionosphere is defined as 0.5 jump, whereas the path with a first reflection from the ionosphere to the ocean surface and subsequent return from the sea surface to the ionosphere then to the radar receiving system is denoted as 1 jump. Therefore, the ionospheric echoes for HFSWR may also involve 0.5 jump, 1 jump, 2 jumps, etc. Fig. 2 shows the possible propagation paths for ionospheric echoes.

Here, the ionospheric echoes from the E-layer in the RD spectrum may originate from a mixed path or 0.5 jump. In the following, from a simple geometric analysis, we can conclude that these echoes are associated with oblique propagation.

If the ionospheric echoes originate from a mixed path, we can obtain the following equation based on the geometric relationship of the propagation path:

$$(\tan\theta + \sec\theta)h = R \tag{1}$$

where h and R represent the vertical distance and radial distance from radar to ionosphere. The range of incident angles θ can be obtained according to h and R in the RD spectrum and the ionosonde, respectively. Here, we found the incidence angle falls in the range of

$$20^\circ \leq \theta \leq 24^\circ. \tag{2}$$

According to the secant theorem, the range of f_0 E corresponding to this incidence angle range can be determined as follows:

$$5.3\ \text{MHz} \leq f_0 = f_0\text{E} \cdot \sec\theta \leq 5.5\ \text{MHz}. \tag{3}$$

Since the operating frequency of the radar is 6 MHz, the radar signal should penetrate the E-layer at this incident angle. However, this presents a contradiction.

If the ionospheric echoes are from the direct path of oblique backscattering in the E-layer, we can obtain (4) based on the geometry of the path

$$h = R\cos\theta. \tag{4}$$

Therefore, the range of incidence angles can be estimated by h as follows:

$$47^\circ \leq \theta \leq 50^\circ. \tag{5}$$

According to the secant theorem, the range of f_0E corresponding to this incidence angles is as follows:

$$7.3\ \text{MHz} \leq f_0 = f_0\text{E} \cdot \sec\theta \leq 7.7\ \text{MHz}. \tag{6}$$

Since the radar operating frequency 6 MHz is lower than the critical frequency, backscattering will occur, which verifies that the ionospheric echoes in the RD spectrum originate from the backscattering propagation path in the E-layer (0.5 jump).

B. HFSWR Beams Split Into O-Trace and X-Trace

According to the electromagnetic theory of HF wave propagation in the ionosphere, incident HF waves can be divided into an O-trace and an X-trace when the geomagnetic field is considered. For ionosonde and a specific ionosphere layer, the calculated ionospheric critical frequency is based only on the O-trace as well as the inverted values of the real reflection height and electron density profile. If the radar operating frequency is higher than the critical frequency of the O-trace and lower than the critical frequency of the X-trace, no ionospheric echoes

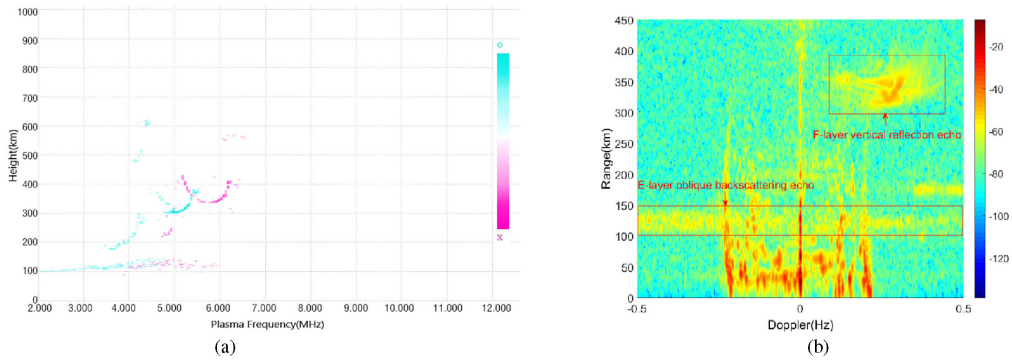

Fig. 3. Comparison between the ionogram and RD spectrum at 10:38 A.M. on June 28, 2018. (a) Ionogram. (b) RD spectrum of HFSWR.

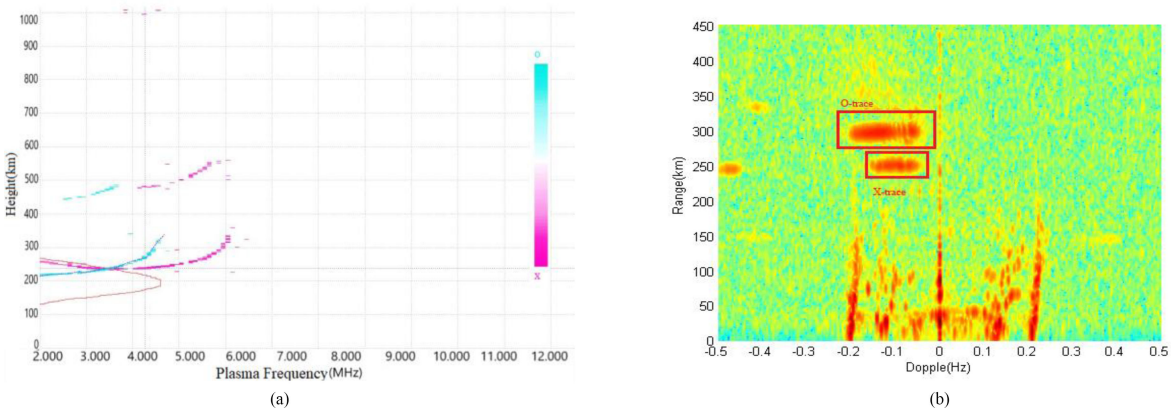

Fig. 4. Comparison between the ionograms and RD spectrums at 16:05 P.M. on January 5, 2019. (a) Ionogram. (b) RD spectrum of HFSWR.

should appear in the vertical reflection according to the inversion method of the ionosonde. However, this is not consistent with the observation of HFSWR.

Fig. 3 shows the measured data from HFSWR and ionosonde in Weihai at 10:38 A.M. on June 28, 2018. From the ionogram in Fig. 3(a), according to the O-trace, the critical frequencies of the E-layer and F-layer are 4.8 and 5.5 MHz, respectively. Fig. 3(b) shows the Doppler frequency spread of ionospheric echoes in the range 100–150 km. For this range, these echoes should originate from the oblique skywave path in the E-layer when the radar operating frequency is 6 MHz. Furthermore, the ionospheric echoes at 320–370 km should come from vertical reflections in the F-layer. Corresponding to the ionogram, the virtual reflection height of 6 MHz is approximately 340 km. Due to the long coherent processing interval, the RD spectrum and ionogram are roughly consistent in this range. Moreover, the Doppler spread distribution of ionospheric echoes should be related to the drift of ionospheric irregularities. Based on the ionosonde inversion algorithm, f_0F2 is equal to the maximum frequency of the O-trace (5.5 MHz). The radar operating frequency (6 MHz) already exceeds f_0F2 (5.5 MHz), but ionospheric echoes are still evident in the RD spectrum. Therefore, for a specific layer of ionosphere, the critical frequency of the ionosphere observed by HFSWR corresponds to the maximum of the O-trace and X-trace frequencies, while ionosonde always picks up the O-trace component.

Fig. 4 shows the measured data from HFSWR and Ionosonde at 16:05, January 5, 2019 in Weihai. The operating frequency of the radar is 4.1 MHz. Fig. 4(a) shows that for 4.1 MHz, the virtual height of X-trace reflection is about 238 km and that of O-trace reflection is about 270 km. According to the RD spectrum of Fig. 4(b), the reflection virtual heights of the X-trace and O-trace are 245–260 km and 285–310 km respectively. The result from Fig. 4 also confirms the aforementioned conclusion about the O-trace and X-trace phenomena.

C. Relationship Between Range-Folded Ionospheric Echoes and Variation in Ionosphere Layer

Figs. 4 and 5 illustrate the ionograms and RD spectra of HFSWR, respectively, on the morning of January 5, 2019. The corresponding times are 11:55 A.M., 12:27 P.M., 12:39 P.M., and 12:51 P.M. The radar operating frequency is 4.1 MHz. According to the ionograms generated during this period, the E-layer disappears. Thus, the main ionospheric echoes are from the F-layer, and the peak electron density of the F-layer shows a trend of decreasing with time. The ionospheric characteristic parameters from the ionograms are shown in Table II.

Fig. 4(a) shows that the ionospheric echoes at 4.1 MHz will split into an X-trace and an O-trace at the heights of 230 and 270 km, respectively. Meanwhile, Fig. 5(a) displays the ionospheric echoes appearing at 230–240 km and 270–280 km. The

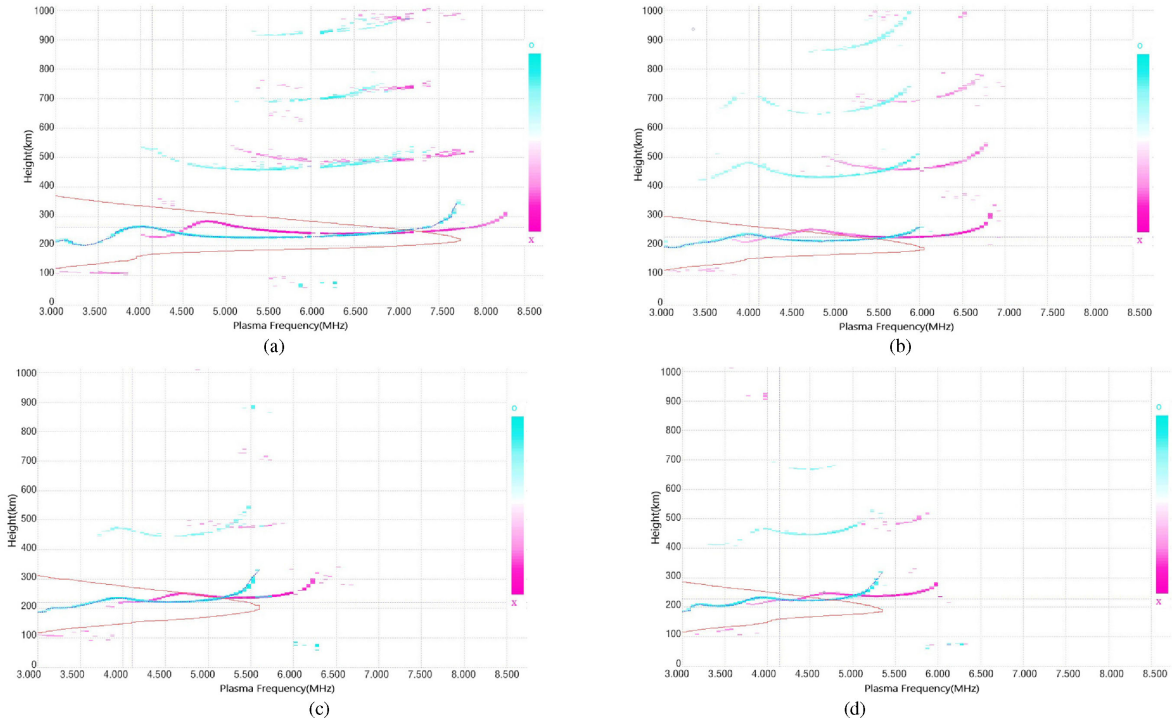

Fig. 5. Ionograms on January 5, 2019; location: Weihai. (a) 11:55 A.M., (b) 12:27 P.M., (c) 12:39 P.M., (d) 12:51 P.M.

TABLE II
IONOSPHERIC CHARACTERISTICS FROM IONOGRAMS

Label	11:55	12:27	12:39	12:51
f_0F2	7.700 MHz	6.000 MHz	5.550 MHz	5.300 MHz
f_0F1	3.950 MHz	3.900 MHz	4.100 MHz	4.000 MHz
hF2	230 km	215 km	222 km	222 km
hF1	202 km	195 km	187 km	185 km
M3000F2	3.760	4.008	3.895	3.930
M3000F1	3.939	4.204	4.228	4.204
fxI	8.300 MHz	6.600 MHz	6.149 MHz	5.899 MHz
fmin	3.000 MHz	3.000 MHz	3.000 MHz	3.000 MHz
hmF2	220 km	189 km	204 km	188 km
hmF1	165 km	152 km	156 km	153 km
hmE	110 km	110 km	110 km	110 km
ymF2	46 km	31 km	72 km	34 km
ymF1	53 km	37 km	35 km	39 km
ymE	25 km	25 km	25 km	25 km

f0F2, f0 F1, f0Es, f0E, hF2, hF1, hEs, hE, M3000F2, M3000F1, and fxI, fmin are obtained directly from the ionograms. hmF2, hmF1, hmE, ymF2, ymF1, and ymE are the inversion results.

same virtual heights for these two groups of ionospheric echoes indicate that the ionospheric echoes of HFSWR may originate from vertical reflections in the F-layer. This finding confirms that the X-trace and O-trace can be observed in the HFSWR, as analyzed previously.

Here, we focus on the analysis of Fig. 5(c). The ionospheric echoes appear mainly in the range 230–250 km from the F-layer. Combined with the corresponding ionogram presented in Fig. 4(c), the E-layer disappears at 12:39 P.M., and the ionograms indicate that the ionosphere was stable. The virtual reflection height of 4.1 MHz is 230 km, indicating that the main ionospheric echoes in the RD spectrum originate from vertical reflections in the F2-layer. This ionospheric distribution is different from that at the other three times and shows a more complex spatial ionospheric structure. Expanded strips of ionospheric echoes appear at the ranges of approximately 35, 100, 150, and 250 km with relatively weak intensities, indicating range-folded paths. Compared with the inversion results of the

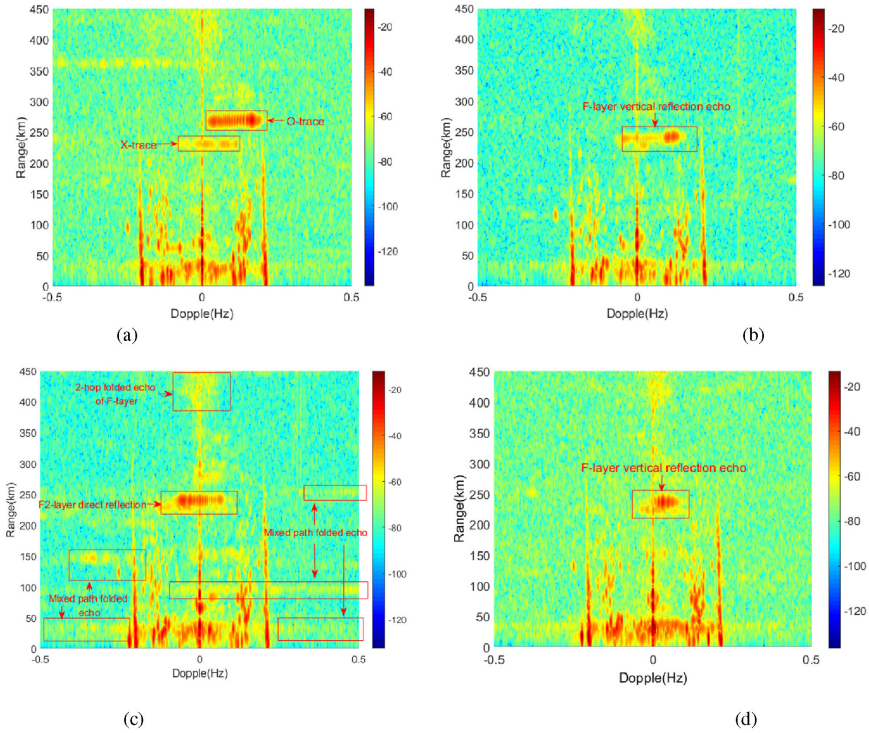

Fig. 6. RD spectrums of HFSWR on January 5, 2019; location: Weihai. (a) 11:55 A.M., (b) 12:27 P.M., (c) 12:39 P.M., (d) 12:51 P.M.

ionograms at 12:27 P.M. and 12:51 P.M., the thickness of the F2-layer at 12:39 P.M. is 72 km, twice as that at 12:27 P.M. and 12:51 P.M. Thus, we may claim that these ionospheric echoes are caused by the short-term thickening of the F2-layer. Besides, we further suppose that the relatively weak intensities of the aforementioned range-folded ionospheric echoes may be caused by a sudden change in the ionospheric structure in the F2-layer. As a result of this abrupt variation, the ionospheric echoes of the preceding range period traveling along the skywave path or mixed path are folded into the current range. Otherwise, ionospheric echoes should not exist at 35 km for the HF band signal.

Moreover, the most significant observation of the ionosphere throughout Fig. 4(a)–(d) is that f_0F2 decreases from 7.7 to 5.3 MHz from 11:55 A.M. to 12:51 P.M. However, the variation in corresponding RD spectra of HFSWR is not so obvious. Thus, we analyze the max, mean, standard deviation, and entropy of amplitude of four ionospheric echoes in the RD spectra from 100 to 450 km, as shown in Fig. 7. The horizontal axis represents the time beginning at 11:55 A.M. (origin), and the vertical axis is the amplitude of the four ionospheric echoes in the RD spectrums (dB). The standard deviation at 12:39 P.M. (the third point) exceeds those at 12:27 P.M. and 12:51 P.M. by nearly 10 dB. This means the ionospheric echoes in the RD spectrum of HFSWR have strong fluctuation at that time.

Furthermore, combining Fig. 3 through Fig. 6 reveals that the range of F-layer echoes (above 150 km) in the RD spectrum is roughly consistent with the virtual height of the ionogram, while the range of E-layer echoes is quite different. This indicates that the F-layer echoes of HFSWR may come from the vertical

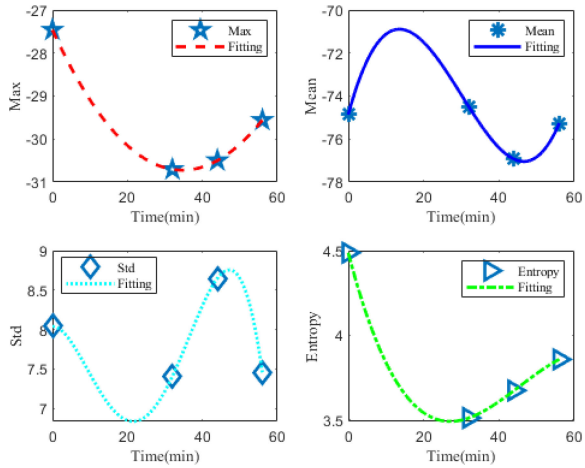

Fig. 7. Diagram of the various RD spectrums during the morning of January 5, 2019; location: Weihai.

propagation path, which is also consistent with previous observations [33]. On the contrary, the E-layer echoes in HFSWR that do not match the virtual height of the ionogram may originate from other propagation paths. Some studies have considered that E-layer echoes may come from the mixed path rather than the vertical reflected path. Here, we think that these E-layer echoes may also come from the path of oblique skywave propagation.

IV. Conclusion

In this article, the preliminary observation and analysis results of ionosphere characteristics using a digital ionosonde and an

HFSWR at the mid-latitude of China have been presented. The main conclusions include the following.

1) We confirmed the existence of skywave propagation paths for the ionospheric echoes of HFSWR in addition to the vertical reflection path and the ionosphere-ocean mixed path. Moreover, the skywave propagation path provides HFSWR with the possibility to achieve OTH detection like an OTHR.
2) HFSWR beams can be divided into two types (O-trace and X-trace) according to the reflections in ionosphere. For a specific layer of ionosphere, the critical frequency of the ionosphere observed by HFSWR corresponds to the maximum of the O-trace and X-trace frequencies. However, ionosonde always uses the maximum O-trace frequency as the critical value. Additionally, HFSWR can also detect the drift of ionosphere irregularities.
3) Range-folded ionospheric echoes with strong fluctuation appear in HFSWR spectra as the result of short-term thickening of the F2-layer. Due to the presence of range-folded ionospheric echoes, new ionospheric clutter suppression algorithms should be developed for such echoes to improve radar detection and remote sensing performance. Moreover, the F-layer echoes of HFSWR may come from the vertical propagation path, while the E-layer echoes may originate from the oblique skywave propagation path.

Through this study, it shows that coordinated observation using HFSWR and ionosondes can provide better knowledge of the ionosphere characteristics. It should be noted that the above conclusions are all derived based on the analysis of limited data. Consequently, further validation of these preliminary findings and their underlying physical mechanism should be undertaken once an extensive dataset is available.

REFERENCES

[1] C. G. Nova and A. Reineix, "Method for the sea clutter characterization in HF surface wave radars from the fields diffracted by the sea surface," *IEEE J. Sel. Topics Appl. Earth Observ. Remote Sens.*, vol. 13,, no. 11, pp. 403–413, Jan. 2020.

[2] J. Zhao, Y. Tian, B. Wen, and Z. Tian, "Unambiguous wind direction field extraction using a compact shipborne high-frequency radar," *IEEE Trans. Geosci. Remote Sens.*, to be published.

[3] W. Sun *et al.*, "A vessel azimuth and course joint re-estimation method for compact HFSWR," *IEEE Trans. Geosci. Remote Sens.*, vol. 58,, no. 2, pp. 1041–1051, Feb. 2020.

[4] J. Cai, H. Zhou, W. Huang, and B. Wen, "Ship detection and direction finding based on time-frequency analysis for compact HF radar," *IEEE Geosci. Remote Sens. Lett.*, to be published.

[5] Y. Tian, Z. Tian, J. Zhao, B. Wen, and W. Huang, "Wave height field extraction from first-order doppler spectra of a dual-frequency wide-beam high-frequency surface wave radar," *IEEE Trans. Geosci. Remote Sens.*, vol. 58,, no. 2, pp. 1017–1029, Feb. 2020.

[6] D. Barrick, "First-order theory and analysis of MF/HF/VHF scatter from the sea," *IEEE Trans. Antennas Propag.*, vol. 20, no. 1, pp. 2–10, Jan. 1972.

[7] L. Sevgi, A. Ponsford, and H. C. Chan, "An integrated maritime surveillance system based on high-frequency surface-wave radars. I. Theoretical background and numerical simulations," *IEEE Antennas Propag. Mag.*, vol. 43, no. 4, pp. 28–43, Aug. 2001.

[8] H. Chan, "Characterization of ionospheric clutter in HF surfacewave radar," DRDC Ottawa, Ottawa, ON, Canada, Tech. Rep. 2003-114, Sep. 2003.

[9] Y. Guo, Y. Wei, R. Xu, and L. Yu, "New BSS-based ABF for heterogeneous ionospheric clutter mitigation in HFSWR," *IET Radar Sonar Navig.*, vol. 13, no. 11, pp. 2015–2023, 2019.

[10] J. Zhang, W. Deng, X. Zhang, M. Zhao, and Q. Yang, "A method of track matching based on multipath echoes in high-frequency surface wave radar," *IEEE Antennas Wireless Propag. Lett.*, vol. 17, no. 10, pp. 1852–1855, Oct. 2018.

[11] X. Zhang, Q. Yang, D. Yao, and W. Deng, "Main-lobe cancellation of the space spread clutter for target detection in HFSWR," *IEEE J. Sel. Topics Signal Process.*, vol. 9, no. 8, pp. 1632–1638, Dec. 2015.

[12] W. Wang and L. Wyatt, "Generalised noise cancellation method for wave estimation by HF surface wave radar," *IET Radar Sonar Navig.*, vol. 8, no. 6, pp. 622–631, Jul. 2014.

[13] S. Shang, Z. Ning, and L. Yang, "A new method for ionospheric clutter suppression in HFSWR," in *Proc. IEEE CIE Int. Conf. Radar*, Oct. 2011, pp. 141–144.

[14] F. Jangal, S. Saillant, and M. Hélier, "Ionospheric clutter mitigation using one-dimensional or two-dimensional wavelet processing," *IET Radar Sonar Navig.*, vol. 3, no. 2, pp. 112–121, Jan. 2009.

[15] X. Guo, H. Sun, and T. S. Yeo, "Interference cancellation for high-frequency surface wave radar," *IEEE Trans. Geosci. Remote Sens.*, vol. 46, no. 7, pp. 1879–1891, Jul. 2008.

[16] H. Zhou, B. Wen, and S. Wu, "Ionospheric clutter suppression in HFSWR using multilayer crossed-loop antennas," *IEEE Geosci. Remote Sens. Lett.*, vol. 11, no. 2, pp. 429–433, Feb. 2014.

[17] Z. Chen, F. Xie, C. Zhao, and C. He, "An orthogonal projection algorithm to suppress interference in high-frequency surface wave radar," *Remote Sens.*, vol. 10, no. 3, Mar. 2018, Art. no. 403.

[18] H. Gao, G. Li, Y. Li, Z. Yang, and X. Wu, "Ionospheric effect of HF surface wave over-the-horizon radar," *Radio Sci.*, vol. 41, no. 6, pp. 1–10, Nov. 2006.

[19] H. Zhou, B. Wen, and S. Wu, "Ionosphere probing with a high frequency surface wave radar," *Prog. Electromagn. Res.*, vol. 20, no. 1, pp. 203–214, Mar. 2011.

[20] X. Yang, A. Liu, C. Yu, and L. Wang, "Ionospheric Clutter model for HF Sky-wave path propagation with an FMCW source," *Int. J. Antennas Propag.*, vol. 2019, no.May 2019, Art. no. 1782942.

[21] X. Yang, C. Yu, A. Liu, L. Wang, and T. Quan, "The vertical ionosphere parameters inversion for high frequency surface wave radar," *Int. J. Antennas Propag.*, vol. 2016, Dec. 2016, Art. no. 8609372.

[22] T. Thayaparan and J. MacDougall, "Evaluation of ionospheric sporadic-E clutter in an arctic environment for the assessment of high-frequency surface-wave radar surveillance," *IEEE Trans. Geosci. Remote Sens.*, vol. 43, no. 5, pp. 1180–1188, May 2005.

[23] J. Walsh, E. W. Gill, W. Huang, and S. Chen, "On the development of a high-frequency radar cross section model for mixed path ionosphere–ocean propagation," *IEEE Trans. Antennas Propag.*, vol. 63, no. 6, pp. 2655–2664, Jun. 2015.

[24] S. Chen, W. Huang, and E. W. Gill, "A vertical reflection ionospheric clutter model for HF radar used in coastal remote sensing," *IEEE Antennas Wireless Propag. Lett.*, vol. 14, no. 1, pp. 1689–1693, Apr. 2015.

[25] S. Chen, E. W. Gill, and W. Huang, "A first-order HF radar cross-section model for mixed-path ionosphere–ocean propagation with an FMCW source," *IEEE J. Ocean. Eng.*, vol. 41, no. 4, pp. 982–992, Oct. 2016.

[26] S. Chen, E. W. Gill, and W. Huang, "A high-frequency surface wave radar ionospheric clutter model for mixed-path propagation with the second-order sea scattering," *IEEE Trans. Antennas Propag.*, vol. 64, no. 12, pp. 5373–5381, Dec. 2016.

[27] M. Zhao, X. Zhang, Q. Yang, and W. Deng, "Using sky-wave echoes information to extend HFSWR's maximum detection range," *Radio Sci.*, vol. 53, no. 8, pp. 922–932, Aug. 2018.

[28] M. Zhao, X. Zhang, Q. Yang, and J. Zhang, "Coverage area analysis of combined sky-wave and surface-wave monostatic high frequency radar," *IEEE Access*, vol. 7, pp. 91427–91434, 2019.

[29] M. Zhao, X. Zhang, and Q. Yang, "Modified multi-mode target tracker for high-frequency surface wave radar," *Remote Sens.*, vol. 10, no. 7, pp. 1061–1077, Jul. 2018.

[30] R. J. Riddolls, "Modification of a high frequency radar echo spatial correlation function by propagation in a linear plasma density profile," Defence R&D Canada, Ottawa, ON, Canada, Tech. Rep. TM 2011-219, Dec. 2011.

[31] M. Ravan, R. Riddolls, and R. Adve, "Ionospheric and auroral clutter models for HF surface wave and over-the-horizon radar systems," *Radio Sci.*, vol. 47, no. 3, pp. 1–12, Jun. 2012.

[32] M. Ravan and R. S. Adve, "Ionospheric clutter model for high frequency surface wave radar," in *Proc. IEEE Radar Conf.*, Jun. 2012, pp. 0377–0382.

[33] S. Chen, "Ionospheric clutter models for high frequency surface wave radar," Ph.D. dissertation, Memorial Univ. Newfoundland, St. John's, NL, USA, May 2017.
[34] A. M. Ponsford, L. Sevgi, and H. C. Chan, "An integrated maritime surveillance system based on high-frequency surface-wave radars. 2. Operational status and system performance," *IEEE Antennas Propag. Mag.*, vol. 43, no. 5, pp. 52–63, Oct. 2001.

Xuguang Yang received the B.S. and M.S. degrees in mathematics from the Harbin Institute of Technology, Harbin, China, in 2005 and 2007, respectively, and the Ph.D. degrees in electronic engineering from the Harbin Institute of Technology, Harbin, China, in 2019.

He is currently a Professor with the School of Information Engineering, Long Dong University, Qingyang, China. His research interests include the ocean and ionosphere remote sensing from high-frequency surface wave radar, and the reaction-diffusion equations with applications in pattern formations.

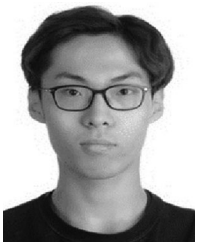

Mingjie Wang was born in Qingyang, China, in June 1998. He is currently working toward the B.S degree in information engineering in Long Dong University, Qingyang, China.

His research interests include computer vision, machine learning, and data mining.

Weimin Huang (Senior Member, IEEE) received the B.S., M.S., and Ph.D. degrees in radio physics from Wuhan University, Wuhan, China, in 1995, 1997, and 2001, respectively, and the M.Eng. degree in engineering electromagnetics from the Memorial University of Newfoundland, St. John's, NL, Canada, in 2004.

He received the Postdoctoral Fellowship from Memorial University of Newfoundland. From 2008 to 2010, he was a Design Engineer with Rutter Technologies, St. John's. Since 2010, he has been with the Faculty of Engineering and Applied Science, Memorial University of Newfoundland, where he is currently a Professor. He has authored more than 250 research articles. His research interests include the mapping of oceanic surface parameters via high-frequency ground wave radar, X-band marine radar, and global navigation satellite systems.

Dr. Huang has been a Technical Program Committee Member. He was a recipient of the IEEE Geoscience and Remote Sensing Society 2019 Letters Prize Paper Award and the Discovery Accelerator Supplements Award from the Natural Sciences and Engineering Research Council of Canada, in 2017. He served as the Technical Program Co-Chair for the IEEE Newfoundland Electrical and Computer Engineering Conference, in 2012 and 2013. He is currently an Associate Editor of IEEE ACCESS and the IEEE CANADIAN JOURNAL OF ELECTRICAL AND COMPUTER ENGINEERING and an Editorial Board Member of *Remote Sensing*. He was a regular Reviewer for more than 50 international journals and a Reviewer for many IEEE International Conferences, such as Radar Con, International Conference on Communications, Globecom, Igarss, and Oceans.

Changjun Yu received the B.S. degree in electronic engineering from the Harbin Institute Technology, Harbin, China, in 1984, and the M.S. and Ph.D. degrees in information and communication engineering from Harbin Engineering University, Harbin, in 1990 and 2010, respectively.

He is currently a Professor with the School of Information and Electrical Engineering, Harbin Institute of Technology at Weihai, Weihai, China. His research interests include high-frequency surface wave radar system design and analysis, target detection, estimation and tracing, and ionosphere remote sensing.